JACS
JOURNAL OF THE AMERICAN CHEMICAL SOCIETY
Article
Cite This: J. Am. Chem. Soc. 2020, 142, 1548−1555
pubs.acs.org/JACS

Molecule Isomerism Modulates the Diradical Properties of Stable Singlet Diradicaloids

Joshua E. Barker,[†] Justin J. Dressler,[†] Abel Cárdenas Valdivia,[‡] Ryohei Kishi,[§] Eric T. Strand,[†] Lev N. Zakharov,[∥] Samantha N. MacMillan,[¶] Carlos J. Gómez-García,[⊥] Masayoshi Nakano,*[,§,□,○,#] Juan Casado,*[,‡] and Michael M. Haley*[,†,△]

[†]Department of Chemistry & Biochemistry and the Materials Science Institute, University of Oregon, Eugene, Oregon 97403-1253, United States

[‡]Department of Physical Chemistry, University of Malaga, Campus de Teatinos s/n 29071 Malaga, Spain

[§]Department of Materials Engineering Science, Graduate School of Engineering Science, Osaka University, Toyonaka, Osaka 560-8531, Japan

[∥]CAMCOR, University of Oregon, Eugene, Oregon 97403-1433, United States

[¶]Department of Chemistry & Chemical Biology, Cornell University, Ithaca, New York 14853, United States

[⊥]Department of Inorganic Chemistry and Instituto de Ciencia Molecular, Universidad de Valencia, 46980 Paterna, Spain

[□]Center for Spintronics Research Network, Graduate School of Engineering Science, Osaka University, Toyonaka, Osaka 560-8531, Japan

[○]Quantum Information and Quantum Biology Division, Institute for Open and Transdisciplinary Research Initiatives, Osaka University, Toyonaka, Osaka 560-8531, Japan

[#]Institute for Molecular Science, 38 Nishigo-Naka, Myodaiji, Okazaki 444-8585, Japan

[△]Phil and Penny Knight Campus for Accelerating Scientific Impact, University of Oregon, Eugene, Oregon 97403-6231, United States

Supporting Information

ABSTRACT: Inclusion of quinoidal cores in conjugated hydrocarbons is a common strategy to modulate the properties of diradicaloids formed by aromaticity recovery within the quinoidal unit. Here we describe an alternative approach of tuning of diradical properties in indenoindenodibenzothiophenes upon *anti* → *syn* isomerism of the benzothiophene motif. This alters the relationship of the S atom with the radical center from linear to cross conjugation yet retains the same 2,6-naphtho conjugation pattern of the rearomatized core. We conduct a full comparison between the *anti* and *syn* derivatives based on structural, spectroscopic, theoretical, and magnetic measurements, showing that these systems are stable open-shell singlet diradicaloids that only access their triplet state at elevated temperatures.

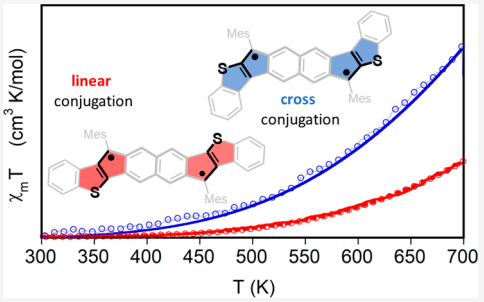

INTRODUCTION

The subject of open-shell character and its interplay with the fundamental properties in polycyclic hydrocarbons[1] is a topic of high relevance to organic electronics.[2] Among molecules possessing open-shell character, diradicals[3] in particular have garnered substantial attention, as they have been proposed as candidates for a variety of materials applications, such as ambipolar organic field effect transistors, singlet fission in organic photovoltaics, and organic spintronics.[4] The design of Kekuléan diradicals is mainly based on a quinoidal core that upon recovery of aromaticity stabilizes the open-shell form (Figure 1).[5] Depending upon the length of the quinoidal motif, the diradical character index (y)[6] and its closely related observable property, the singlet−triplet energy gap (ΔE_{ST}), can be broadly modulated. Though there are other structural features, such as the presence of donor and acceptor groups[7] and the flexibility of the rearomatized core,[8] this quinoidal strategy represents the first and simplest method for tuning the electronic and magnetic properties of diradicaloids and has resulted in a wide range of ΔE_{ST} values in the literature.[5] Adherence to this strategy has resulted in a shotgun approach focused on the synthesis of diversiform quinoidal topologies for the design of Kekuléan diradicaloids.[5] A more deliberate tactic for tuning ΔE_{ST} requires consideration of additional electronic factors that could provide further improvement of the broader quinoidal strategy. We posit that a "structure refinement approach", based on subtle/minor alteration of

Received: November 4, 2019
Published: December 26, 2019

DOI: 10.1021/jacs.9b11898
J. Am. Chem. Soc. 2020, 142, 1548−1555

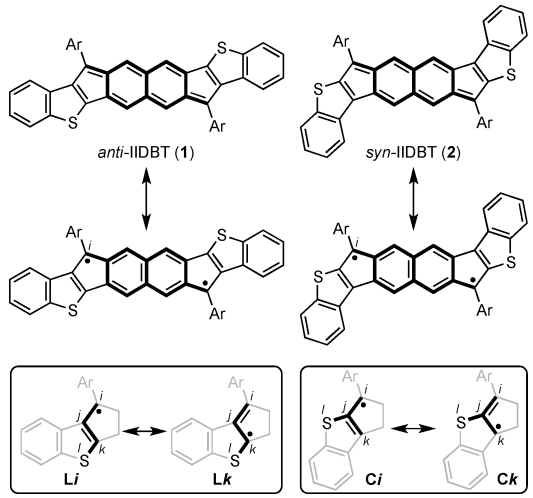

Figure 1. Chemical structures of *anti*-IIDBT (**1**) and *syn*-IIDBT (**2**). All canonical forms possess 2,6-naphtho conjugation (bold bonds). In boxes, linear conjugation (left, **L*i*** and **L*k***) vs cross conjugation (right, **C*i*** and **C*k***) dispositions of the labeled *ijkl* atoms where delocalization of the radical centers to the *k* atoms disrupts thiophene aromaticity.

molecular geometry yet with retention of the same quinoidal/diradical core might allow a more rational modulation of ΔE_{ST}.

We recently reported the *anti*-indenoindenodibenzothiophene diradicaloid **1** (*anti*-IIDBT, Figure 1)[9] with a medium−large *y* value (0.61; PUHF/6-311G* level of theory) and a large ΔE_{ST} (−8.0 kcal mol^{-1}; experimental magnetic susceptibility measurements). Theoretical examination of the molecular parameters involved in the $y-\Delta E_{ST}$ connection found that the position of the sulfur atom (i.e., its lone π-electron pair) relative to the radical center plays a key role increasing ΔE_{ST} at constant *y*. Analysis of the *syn*-IIDBT (**2**) regioisomer therefore became necessary to confirm the theoretical predictions. In the IIDBTs *anti*- and *syn*- denote the position of the sulfur atom relative to the apical carbon (carbon *i*, Figure 1) of the five-membered ring, where the radical can delocalize from *i* to atom *k* in each isomer (canonical forms **L*i*−L*k*** and **C*i*−C*k***). It is important to note that the 2,6-naphtho conjugation path of the radicals is consistent in both **1** and **2**, enabling direct comparison of the effects of the sulfur positioning. Linear conjugation of the sulfur and the radical along the path *ijkl* (**L*i*** and **L*k***) in **1** is in contrast to cross-conjugation along *ijk* in **2** (**C*i*** and **C*k***), and in forms **L*k*** and **C*k*** the thiophene aromaticity is broken, all of which highlight the changing role of the sulfur to act electronically on the radical centers. As a result, this scenario could offer the desired "tuning" of ΔE_{ST} consisting of (i) the relative through-bond separation between the sulfur and the radical center that are three and one atoms apart in **L*i*** and **L*k*** (Figure 1, **1**) compared to two atoms apart in **C*i*** and **C*k*** (Figure 1, **2**) and (ii) the change in the conjugation mode (linear vs cross) between the S lone pair and the radical as discussed above.

Previously reported carbon-based diradicaloid regioisomers have illustrated stark differences in properties that result from making small geometric changes to a molecule; however, in most of these existing cases, structural isomerism concomitantly changes the conjugation pattern, thus altering the diradical character based on the quinoidal character of the molecule.[10] For instance, the known dibenzoheptazethrene isomers (Figure 2) exhibit a marked difference in magnetic

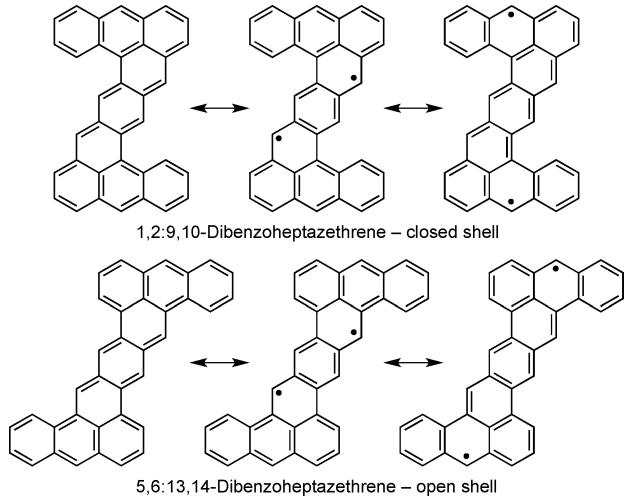

Figure 2. Diradical resonance forms of the hydrocarbon core of the two known dibenzoheptazethrene regioisomers.

properties: whereas the 5,6:13,14-regioisomer displays pronounced open-shell character, the 1,2:9,10-isomer is closed shell.[10d] This difference is exacerbated in the indenofluorene family,[11,12] as there is the possibility of either para, meta, or ortho conjugation between the radical centers (Figure S1), which imparts significant changes in the magnetic structure to the extent that, from one isomer to another, the ground electronic state can even change from singlet to triplet.[11e,13] Furthermore, substituent type and placement on the hydrocarbon backbone very often vary within the isomer series, thus diminishing meaningful comparison of molecule electronic and magnetic properties.[10d,f−i] Structural isomerism in nitrogen- (verdazyl) and oxygen-based (nitroxide) diradicals has also been reported, but in these cases there is little effect on magnetic properties, as the radical centers are not conjugated to the backbone.[14]

Unlike previous examples, the relationship of the radical centers in this current study, namely, 2,6-conjugation, and the bond of benzothiophene fusion (*jk* in Figure 1) are identical in both **1** and **2**, thus meaning that only a single parameter that could influence magnetic properties is altered. Herein we report the synthesis of the *syn*-IIDBT isomers **2a**, **2b**, and **2cH$_2$** as well as new *anti*-IIDBT **1b** (Chart 1) and computationally and experimentally corroborate that varying the benzothio-

Chart 1

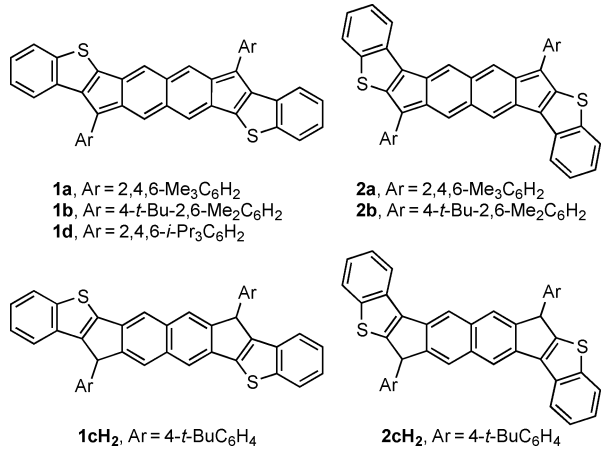

DOI: 10.1021/jacs.9b11898
J. Am. Chem. Soc. 2020, 142, 1548−1555

phene subunit from *anti* to *syn* orientation in the IIDBT scaffold is an efficient strategy to modulate ΔE_{ST}.[6] In addition, we demonstrate that these molecules are stable singlet diradicaloids at room temperature and only access the triplet state at elevated temperatures, where they are stable upward of 375−400 °C.

RESULTS AND DISCUSSION

Computations. Quantum chemical calculations have been performed to explore the validity of our hypothesis. Equation 1 provides, in the two-electron diradical model,

$$\Delta E_{ST} = \frac{U}{2}\left[1 - \frac{1}{\sqrt{y(2-y)}}\right] + 2K_{ab} = \frac{U}{2} f_{ST}(y) + 2K_{ab} \quad (1)$$

the dependence of ΔE_{ST} on y (defined in Equation 2)

$$y = 1 - \frac{1}{\sqrt{1 + \left(\frac{U}{4t_{ab}}\right)^2}} \quad (2)$$

in terms of U (the difference between on- and intersite Coulomb repulsions), t_{ab} (the transfer integral) and K_{ab} (direct exchange integral), where a and b define the electrons in the localized natural orbitals. Table 1 summarizes the main theoretical data for both **1** and **2** (see the Supporting Information for additional details in Table S1).

Table 1. Theoretically Estimated y and ΔE_{ST} Values Together with the Main Physical Parameters

	y[a,b]	ΔE_{ST}[a,c] (kcal mol^{-1})	$U/2$[a,d] (eV)	$\lvert t_{ab}\rvert$[a,d] (eV)	$2K_{ab}$[a,d] (eV)
1	0.613	−8.77	1.563	1.031	0.165
2	0.658	−8.06	1.404	0.905	0.130

[a]Geometry optimization for the singlet/triplet states and frequency analyses were performed at the R- and UB3LYP/6-311G* levels, respectively. [b]Calculated at the PUHF/6-311G* level. [c]Adiabatic ΔE_{ST} value calculated at the spin-flip noncollinear (SF-NC)-TDDFT PBE5050/6-311G* level along with R- or UB3LYP/6-311G* zero-point vibrational energy correction for each spin state. [d]Estimated at the CASCI(2,2)/6-311G* level using the (tuned-)LC-RBLYP MOs (denoted as tuned-LC-RBLYP-CASCI(2,2)/6-311G*). Additional details are given in the Supporting Information.

The computational results reveal that *anti* → *syn* isomerism slightly increases y and decreases ΔE_{ST}, the mechanism of which can be discussed by evaluating the integral parameters (see Table S1 for details of the integral evaluations). For proper disjoint orbitals, such as in our case, $K_{ab} \ll \frac{U}{2} f_{ST}(y)$; hence, according to the values in Table 1, the term containing U and t_{ab} is the dominant factor as far as ΔE_{ST} is concerned. Thus, the increase in U/t_{ab} in **2** (3.10) compared to U/t_{ab} in **1** (3.03) anticipates a moderate increase of y in the *syn* isomer and a concomitant decrease in ΔE_{ST}. The $U_{syn} < U_{anti}$ reveals that the repulsive terms between the radical and the sulfur decrease in **2**, which can be explained by the location of the radical center relative to the sulfur in cross conjugation compared to linear conjugation in **1** (see bold paths in the boxes of Figure 1). In addition, t_{ab}-*syn* < t_{ab}-*anti* is due to enlargement of the interaction distance between the two radicals in the delocalized forms **L*k*** and **C*k***. Form **C*k*** is possible in **2** because of the same cross-conjugation effect, while in the case of **1**, this delocalized form is less feasible due to geminal repulsion between the radical and the sulfur. To further corroborate this description, Figure 3 shows the odd-electron density maps for **1** and **2**, which indicate very little amplitude on the S atom of **2** yet rather large amplitude in the same heteroatom in **1** (see Figure S2 for the HONO/LUNO orbitals and Figure S3 for the Mulliken population analysis). This illustrates the effect of the cross-conjugation mode in the *syn* isomer, which isolates the sulfur from the radical conjugation paths. All these factors contribute to a suitable modulation of ΔE_{ST}, thus fulfilling our purposes in this study.

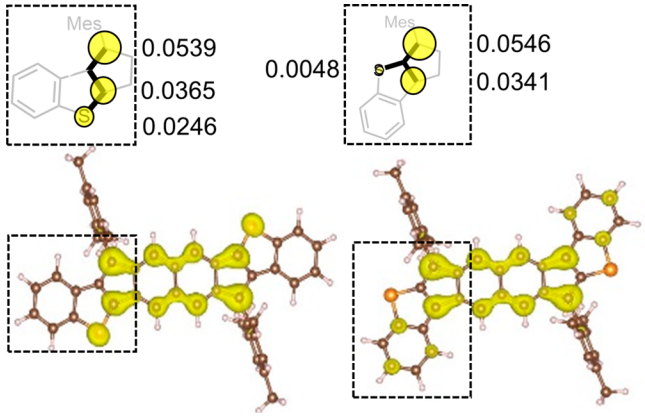

Figure 3. Odd-electron density maps for **1a** (left) and **2a** (right) with contour value 0.0005 au calculated at the tuned-LC-RBLYP-CASCI(2,2)/6-311G* level. Mulliken population analysis for the odd-electron density on the relevant carbon and sulfur atoms of the linear and cross-conjugated paths is shown on top.

In solid-state physics, the Hubbard model[15] successfully accounts for the electronic properties of conductive and semiconducting π-conjugated materials in which two basic electronic parameters are considered among the interacting electrons, namely, the transfer integral, t, and the repulsion term U. One prediction of the model is that the semiconducting energy gap increases with increasing U and decreases with increasing t (a nice case of this U versus t balance is the Mott metal−insulator transition[16]). This description is very similar to that employed in the two-electron model for our case. Here, although t_{ab} is not equal for both isomers, the increase of electronic repulsion U in **1** compared to **2** enlarges the observed magnetic ΔE_{ST} gap on **2** → **1**. This comparison nicely discloses the close correspondence between solid-state physics and molecular physics to address closely related phenomena.

Synthesis. Encouraged by the promising theoretical predictions, the *syn*-IIDBTs **2** were prepared via a similar synthetic route used for **1**. Starting from known bistriflate **3**[17] (Scheme 1), Suzuki−Miyaura cross-coupling with benzothiophene 3-boronpinacolate ester[18] furnished diester **4** in an 87% yield. Saponification of **4** followed by acyl chloride formation and then intramolecular Friedel−Crafts acylation yielded essentially insoluble dione **5**. Reaction of **5** with mesityllithium at −78 °C gave the penultimate diol, which is then reductively dearomatized using $SnCl_2$ in rigorously anaerobic and anhydrous reaction conditions to afford fully conjugated, deep green **2a** in modest yield. Use instead of 2,6-dimethyl-4-*tert*-butylphenyllithium or 4-*tert*-butylphenyllithium gave *syn*-IIDBTs **2b** and **2cH$_2$**, respectively, with the latter structure

DOI: 10.1021/jacs.9b11898
J. Am. Chem. Soc. 2020, 142, 1548−1555

Scheme 1. Synthesis of *syn*-IIDBTs 2

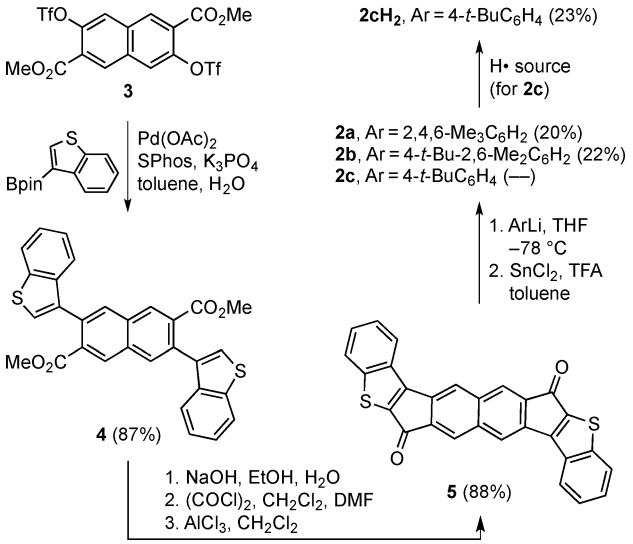

gaining two hydrogen atoms because of the reduced steric protection of the radical centers, in analogy to formation of **1cH$_2$**.[9] Additionally, treatment of the known *anti*-IIDBT dione[9] with 2,6-dimethyl-4-*tert*-butylphenyllithium followed by $SnCl_2$ furnished the new *anti*-IIDBT **1b**.

Solid-State Structure. Dark green crystals suitable for X-ray diffraction were obtained by slow evaporation of a solution of **2b** in a 10:1 mixture of $CHCl_3$ and CH_3CN. The resultant X-ray structure and the relevant experimentally and computationally determined bond lengths for **1** and **2** are given in Figure 4. The X-ray data revealed that the carbon−carbon bond length from the apical carbon to the naphthalene core is 1.419(4) Å, which is comparable in length to the analogous bond in the crystal structures of **1a** (1.424(4) Å)[9] and **1d** (1.426(5) Å; see Figure S5 in the Supporting Information). All three values are roughly the same within experimental error and suggest a pronounced open-shell character of the IIDBT scaffold. In contrast, the analogous CC bond in closed-shell molecules is usually in the range of 1.38−1.40 Å.[11a,c,12b] Interestingly, these ∼1.42 Å values also show that the steric bulk of the aryl group attached to the apical carbon has little to no effect on this bond length (e.g., **1d**), as might be expected given their orthogonality with respect to the plane of the IIDBT framework. The biggest disparity between the structures of **1a**/**d** and **2b** resides in the thiophene rings, where there is a marked difference in the C−S bond lengths, 1.731/1.753 Å for **2b** vs 1.716/1.760 Å for **1a**, reflecting the differences in S orientation, i.e., the linear conjugation vs cross-conjugation arguments. The computational bond lengths do an excellent job replicating the aforementioned trends (Figures 4 and S4 and S5).

In the crystal lattice, **2b** packs as dimeric pairs where one of the outer benzene ring overlaps with the same ring of its nearest neighbor with intermolecular $\pi-\pi$ distances of 3.47−3.51 Å. Although the odd-electron density map in Figure 3 does show finite density on three of the benzene carbons of **2a**, these particular carbons overlap with the three benzene carbons that have negligible density; thus, the likelihood of magnetic interactions between neighboring molecules in the solid state is minimal. This result is in sharp contrast with Kubo's related bisphenalenyl-fused indacene (**6**)[19] and indenoindene (**7**)[20] molecules, which do display multiple

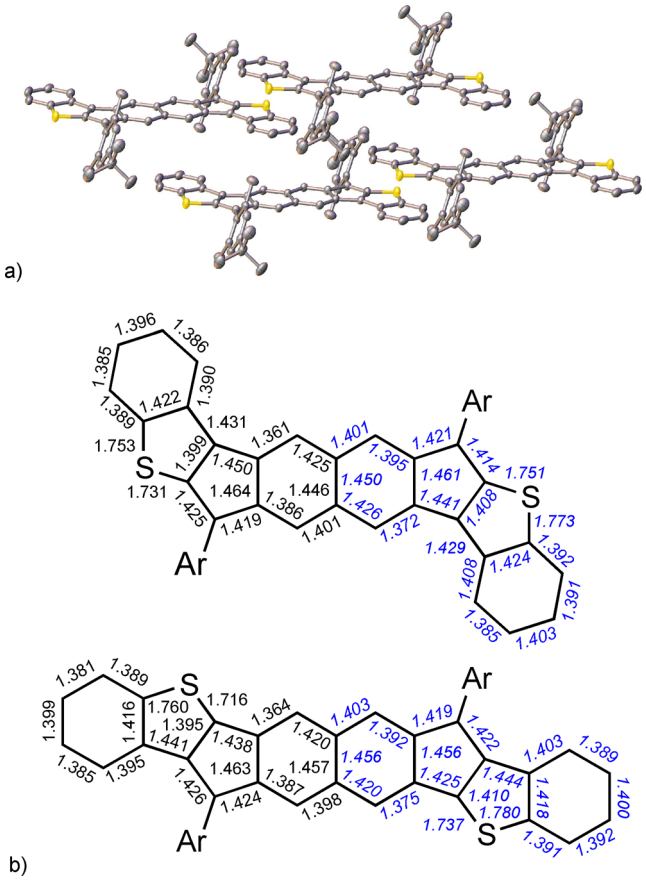

Figure 4. (a) Molecular packing of **2b** with the ellipsoids drawn with 50% probability level; hydrogens are omitted for clarity. (b) Experimental (black) bond lengths for the core motifs of **2b** and **1a** along with the calculated (blue) values for **2a** and **1a**.

close $\pi-\pi$ contacts between carbons of high spin density of the phenalenyl groups (e.g., 3.10−3.23 Å for **7**), suggestive of strong π-dimer formation in the solid state. In the case of **1a** there are only two close $\pi-\pi$ contacts (3.49 and 3.53 Å), whereas in **1d** the analogous distances are all >3.7 Å; however, the outer benzenes possess negligible odd electron density (Figure 3), indicating no intermolecular magnetic interactions are present within these IIDBT scaffolds in the solid state.

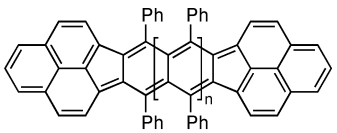

6, n = 0
7, n = 1

Spectroscopic Properties: Absorption and Raman Data. The electronic absorption spectra (Figure 5, top) depict a red-shift of +25 nm from 724 to 749 nm going from **1a** to **2a**, indicating a reduction of the optical gap even though the two compounds are compositionally identical. Quantum chemical calculations (TD-UB3LYP/6-311G* level) also predict a similar red-shift from 703 nm for **1a** to 741 nm for **2a** (see Tables S2 and S3) of the main lowest energy lying theoretical excitation, which corresponds to a HOMO−LUMO transition. In the lowest energy part of these strong absorptions, weak shoulders can also be observed that are typical of diradical molecules and are associated with double excitations. This is

DOI: 10.1021/jacs.9b11898
J. Am. Chem. Soc. 2020, 142, 1548−1555

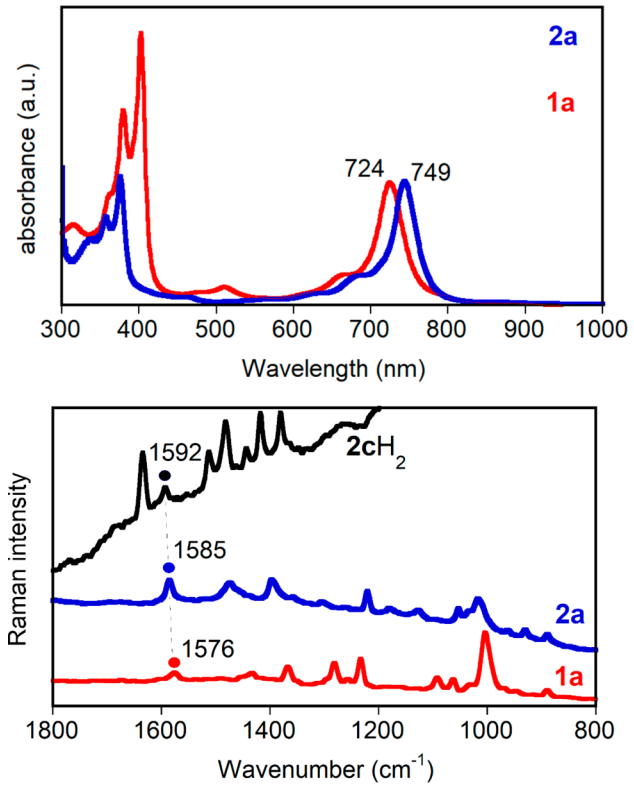

Figure 5. Electronic absorption (in CH_2Cl_2, top) and Raman spectra (in the solid state with 1064 nm laser excitation, bottom) of **1a** (red) and **2a** (blue). Raman spectrum of aromatized **2cH2** is in black.

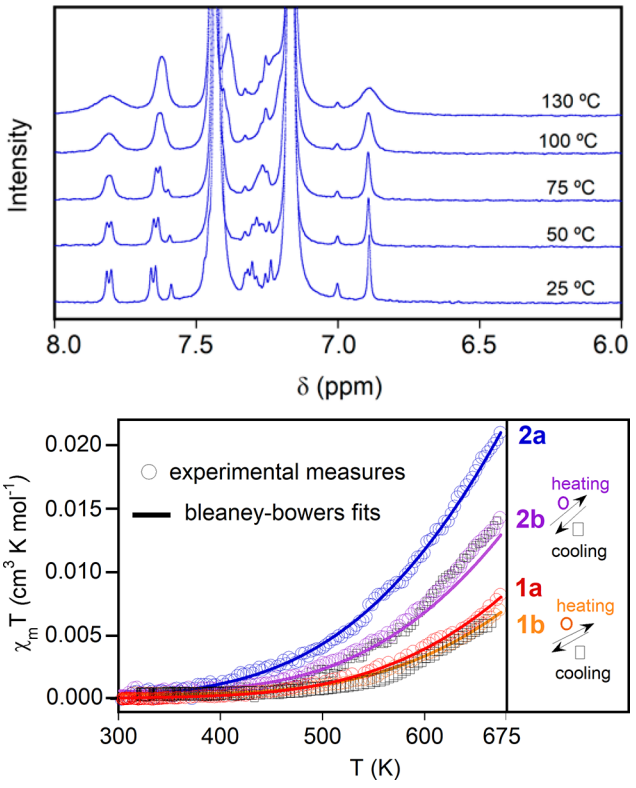

Figure 6. (Top) Variable-temperature ^{1}H NMR spectra (in 1,2-$C_6D_4Cl_2$) of **2a**. (Bottom) SQUID magnetometry data of **1a**,**1b** and **2a**,**2b**; for **1b** and **2b** the data for the heating and cooling curves are denoted by squares and circles, respectively.

related with the t_{ab}-*syn* < t_{ab}-*anti* discussion above, and, as such, it is explained in terms of an extended conjugational path in **2** between the two radical centers due to cross conjugation, which limits the effect of the sulfurs on it.

The solid-state Raman spectra of **1a** and **2a** at room temperature are shown in Figure 5 (bottom). The characteristic C═C stretching mode of the central naphthalene unit in **1a** appears at 1576 cm^{-1} and is representative of a transitional structure from quinoidal to aromatic for this core. This is in agreement with a medium diradical index of y = 0.61, confirming that aromaticity recovery is the main driving force for diradical formation, although it is not fully completed.[5c,9] In the case of **2a** (y = 0.66), the same yet more intense Raman band emerges at 1585 cm^{-1}, upshifted by +9 cm^{-1}, indicating an additional gain of aromatization of the naphthalene core in this isomer. In addition, this band is only +7 cm^{-1} away from the same stretching mode in **2cH$_2$** (1592 cm^{-1}), a molecule that contains a fully aromatized naphthalene (note that in **1a** → **1cH$_2$** the upshift is +11 cm^{-1}). The emerging interpretation is that the contribution of the 2,6-naphthoquinoidal conjugation to ΔE_{ST} does not arise separately from cross-conjugation of the sulfur lone pair and the radical, but there is a synergy between the two. We mean that delocalization of the radical to *k* in form **C*k*** of Figure 1 enlarges/weakens the distance/interaction between the two radicals, which simultaneously reinforces the aromatic character of the central naphthalene.

NMR and SQUID Measurements. The ^{1}H NMR spectra of **2a** as a function of the temperature are shown in Figure 6 (top). At room temperature, the spectrum is clearly resolved with all peaks assignable to the structure of **2a**. At higher temperatures these peaks have broadened, as is clearly observed at 130 °C. While this behavior was observed for **1a**, the onset of peak broadening in **2a** occurs at a considerably lower temperature (75 °C) compared to that for **1a** (125 °C), suggesting a smaller singlet−triplet energy gap.

In the solid state, SQUID measurements for **2a** (Figure 6, bottom) show a clear increase of the magnetic molar susceptibility from low to high temperature that is typical behavior of a singlet low-spin ground electronic state from which a high-spin triplet excited state is populated thermally. Fitting the data to the Bleany−Bowers equation[21] yields a singlet−triplet energy gap of −6.9 kcal mol^{-1}, which agrees well with the ΔE_{ST} predicted from calculations (−8.06 kcal mol^{-1}). Furthermore, the matching of the experimental data to a Bleany−Bowers dimer model confirms the rather small spin−spin intermolecular interaction in the solid such as revealed by the large π−π distances in the X-ray data. This ∼1 kcal mol^{-1} modulation of ΔE_{ST} in **2a** demonstrates the fine tuning of ΔE_{ST} in the closely related IIDBT regioisomers. This result stands in contrast to the much larger range of ΔE_{ST} values that result from variation of the size of the acene diradical core (i.e., the number of fused rings). For example, in the family of bisphenalenyl-fused molecules, ΔE_{ST} varies from −7.2 kcal mol^{-1} for **6** to −4.5 kcal mol^{-1} for **7** and −2.9 kcal mol^{-1} for the analogue possessing an anthracene core.[22]

One of the unique attributes of the IIDBTs is the need for pronounced heating in order to populate the triplet state, which then raises the question of the thermal stability of the scaffold. Thermogravimetric analysis (TGA, Figures S6−S9) of both sets of isomers reveals that the onset of decomposition is ∼375 °C with significant mass loss above 400 °C. Examination of the data for **1a** indicates that the first two events are

DOI: 10.1021/jacs.9b11898
J. Am. Chem. Soc. 2020, 142, 1548−1555

sequential loss of the mesityl groups followed by decomposition of the conjugated core at higher temperatures (>450 °C). Heating samples of **1b** and **2b** in the SQUID up to 675−700 K and then cooling back to room temperature (Figures 6 and S10 and S11) affords ΔE_{ST} values (**1b**: H −8.2/C −8.4 kcal mol^{-1}; **2b**: H −7.2/C −7.0 kcal mol^{-1}) that are in very good agreement with those obtained by only heating SQUID samples of **1a** and **2a** (−8.0 and −6.9 kcal mol^{-1}, respectively), further corroborating the thermal stability of the IIDBT family of diradicaloids.

CONCLUSIONS

In summary, we have demonstrated a finer, rational adjustment of ΔE_{ST} by *anti* → *syn* isomerism of the IIDBT framework. The two constitutional isomers have a common 2,6-naphtho core that contributes the greater amount to ΔE_{ST}, whereas *anti*/*syn* flip modulates this value within ∼1 kcal mol^{-1}, which we attribute to the combination of change in the relative position of the radical and of the S atom together with the change from linear to cross conjugation. Importantly, we have shown that IIDBTs **1** and **2** are stable singlet diradicaloids at room temperature and only access the triplet state at elevated temperatures, where they are stable upward of 375−400 °C, as revealed by TGA as well as by the reversibility of the high-temperature SQUID measurements.

With this study we have posited the question of the necessary fine control of ΔE_{ST} in a stable diradical as the way to design tailored open-shell molecules with control of their emerging properties. While most published studies employ a more qualitative approach to varying ΔE_{ST} without much emphasis on the actual ΔE_{ST} outcome, knowledge of how to subtly tune the singlet−triplet energy gap as well as an understanding of what diradical parameter one is altering will be essential for future design and use of diradicals in materials applications. Practical diradicals are those with intermediate diradical character (i.e., greater stability, efficient nonlinear optical response, capability of photonic control, etc.) where the tailored design of ΔE_{ST} becomes mandatory. Additional efforts to accomplish this tailoring via a "structural refinement approach" will be the subject of future studies.

ASSOCIATED CONTENT

Supporting Information

The Supporting Information is available free of charge at https://pubs.acs.org/doi/10.1021/jacs.9b11898.

Experimental details, ^{1}H and ^{13}C NMR spectra for all new compounds, and computational details including the coordinates of optimized structures (PDF)

X-ray structure of **1d** (CIF)

X-ray structure of **2b** (CIF)

AUTHOR INFORMATION

Corresponding Authors

*mnaka@cheng.es.osaka-u.ac.jp

*casado@uma.es

*haley@uoregon.edu

ORCID

Joshua E. Barker: 0000-0001-6139-8858

Samantha N. MacMillan: 0000-0001-6516-1823

Carlos J. Gómez-García: 0000-0002-0015-577X

Masayoshi Nakano: 0000-0002-3544-1290

Juan Casado: 0000-0003-0373-1303

Michael M. Haley: 0000-0002-7027-4141

Notes

The authors declare no competing financial interest.

ACKNOWLEDGMENTS

This work was supported by the U.S. National Science Foundation (CHE-1565780), by the Spanish Government, MINECO (CTQ2015-69391-P and PGC2018-098533-*b*-100, CTQ2016-80955, and CTQ2017-87201-P), the Generalidad Valencia (Prometeo2019/076), and the Japan Society for the Promotion of Science (JSPS, KAKENHI Grants JP18H01943, JP17H05157, and JP26107004). Mass spectrometry capabilities in the CAMCOR facility are supported by the NSF (CHE-1625529). We thank Dr. Casey Check for his assistance with acquiring and interpreting the TGA data. Theoretical calculations were partly performed using Research Center for Computational Science, Okazaki, Japan.

REFERENCES

(1) Clar, E. *Polycyclic Hydrocarbons*, Vols. *1 and 2*; John Wiley: New York, 1964.

(2) Dediu, V. A.; Hueso, L. E.; Bergenti, I.; Taliani, C. Spin route to organic electronics. *Nat. Mater.* **2009**, *8*, 707−716.

(3) Abe, M. Diradicals. *Chem. Rev.* **2013**, *113*, 7011−7088.

(4) (a) Muhammad, S.; Nakano, M.; Al-Sehemi, A. G.; Kitagawa, Y.; Irfan, A.; Chaudhry, A. R.; Kishi, R.; Ito, S.; Yoneda, K.; Fukuda, K. Role of a singlet diradical character in carbon nanomaterials: a novel hot spot for efficient nonlinear optical materials. *Nanoscale* **2016**, *8*, 17998−18020. (b) Nakano, M. Open-Shell-Character-Based Molecular Design Principles: Applications to Nonlinear Optics and Singlet Fission. *Chem. Rec.* **2017**, *17*, 27−62. (c) Huang, Y.; Egap, E. Open-shell organic semiconductors: An emerging class of materials with novel properties. *Polym. J.* **2018**, *50*, 603−614.

(5) (a) Zeng, Z.; Shi, X.; Chi, C.; Lopez Navarrete, J. T.; Casado, J.; Wu, J. Pro-aromatic and anti-aromatic π-conjugated molecules: an irresistible wish to be diradicals. *Chem. Soc. Rev.* **2015**, *44*, 6578−6596. (b) Shi, X.; Chi, C. Heterocyclic Quinodimethanes. *Top. Curr. Chem.* **2017**, *375*, 169−207. (c) Casado, J. Para-Quinodimethanes: A Unified Review of the Quinoidal-Versus-Aromatic Competition and its Implications. *Top. Curr. Chem.* **2017**, *375*, 209−248. (d) Tobe, Y. Quinodimethanes Incorporated in Non-Benzenoid Aromatic or Antiaromatic Frameworks. *Top. Curr. Chem.* **2018**, *375*, 107−168. (e) Gopalakrishna, T. Y.; Zeng, W.; Lu, X.; Wu, J. From open-shell singlet diradicaloids to polyradicaloids. *Chem. Commun.* **2018**, *54*, 2186−2199.

(6) (a) Nakano, M.; Kishi, R.; Ohta, S.; Takahashi, H.; Kubo, T.; Kamada, K.; Ohta, K.; Botek, E.; Champagne, B. Relationship between Third-Order Nonlinear Optical Properties and Magnetic Interactions in Open-Shell Systems: A New Paradigm for Nonlinear Optics. *Phys. Rev. Lett.* **2007**, *99*, 033001-1−033001-4. (b) Nakano, M.; Champagne, B. Diradical character dependences of the first and second hyperpolarizabilities of asymmetric open-shell singlet systems. *J. Chem. Phys.* **2013**, *138*, 244306-1−244306-13.

(7) (a) Nakano, M.; Minami, T.; Yoneda, K.; Muhammad, S.; Kishi, R.; Shigeta, Y.; Kubo, T.; Rougier, L.; Champagne, B.; Kamada, K.; Ohta, K. Giant Enhancement of the Second Hyperpolarizabilities of Open-Shell Singlet Polyaromatic Diphenalenyl Diradicaloids by an External Electric Field and Donor_Acceptor Substitution. *J. Phys. Chem. Lett.* **2011**, *2*, 1094−1098. (b) Zeng, Z.; Ishida, M.; Zafra, J. L.; Zhu, X.; Sung, Y. M.; Bao, N.; Webster, R. D.; Lee, B. S.; Li, R.-W.; Zeng, W. Y.; Chi, C.; López Navarrete, J. T.; Ding, J.; Casado, J.; Kim, D.; Wu, J. Pushing Extended *p*-Quinodimethanes to the Limit: Stable Tetracyano-oligo(*N*-annulated perylene)quinodimethanes with Tunable Ground States. *J. Am. Chem. Soc.* **2013**, *135*, 6363−6371. (c) Zeng, Z.; Lee, S.; Zafra, J. L.; Ishida, M.; Bao, N.; Webster, R. D.;

DOI: 10.1021/jacs.9b11898
J. Am. Chem. Soc. 2020, 142, 1548−1555

López Navarrete, J. T.; Ding, J.; Casado, J.; Kim, D.-H.; Wu, J. Turning on the biradical state of tetracyano-perylene and quaterrylenequinodimethanes by incorporation of additional thiophene rings. *Chem. Sci.* **2014**, *5*, 3072−3080. (d) Zeng, Z.; Lee, S.; Son, M.; Fukuda, K.; Mayorga Burrezo, P.; Zhu, X.; Qi, Q.; Li, R.-W.; López Navarrete, J. T.; Ding, J.; Casado, J.; Nakano, M.; Kim, D.; Wu, J. Push−Pull Type Oligo(N-annulated perylene)quinodimethanes: Chain Length and Solvent-Dependent Ground States and Physical Properties. *J. Am. Chem. Soc.* **2015**, *137*, 8572−8583.

(8) Zeng, Z.; Sung, Y. M.; Bao, N.; Tan, D.; Lee, R.; Zafra, J. L.; Lee, B. S.; Ishida, M.; Ding, J.; López Navarrete, J. T.; Li, Y.; Zeng, W.; Kim, D.; Huang, K.-W.; Webster, R. D.; Casado, J.; Wu, J. Stable Tetrabenzo-Chichibabin's Hydrocarbons: Tunable Ground State and Unusual Transition between Their Closed-Shell and Open- Shell Resonance Forms. *J. Am. Chem. Soc.* **2012**, *134*, 14513−14525.

(9) Dressler, J. J.; Teraoka, M.; Espejo, G. L.; Kishi, R.; Takamuku, S.; Gómez-García, C. J.; Zakharov, L. N.; Nakano, M.; Casado, J.; Haley, M. M. Thiophene and its sulfur inhibit indenoindenodibenzothiophene diradicals from low-energy lying thermal triplets. *Nat. Chem.* **2018**, *10*, 1134−1140.

(10) Examples of quinoidal/diradicaloid constitutional isomers, *inter alia*: (a) Tukada, H. *p*-Phenylene-2,2′-bis(1,1:3,3-di-2,2′-biphenylenepropenyl): A Stable Non-Kekule Molecule as a Ground-State Singlet. *J. Am. Chem. Soc.* **1991**, *113*, 8991−8992. (b) Tukada, H.; Mutai, K. A Stable Triplet Non-Kekulé Molecule; *m*-Phenylene-2,2′-bis(1,1:3,3-di-2,2′-biphenylenepropenyl). *Tetrahedron Lett.* **1992**, *33*, 6665−6668. (c) Kubo, T.; Sakamoto, M.; Nakasuji, K. Biradicaloid Character of Phenalenyl-Based Aromatic Compounds with a Small HOMO−LUMO Gap. *Polyhedron* **2005**, *24*, 2522−2527. (d) Sun, Z.; Lee, S.; Hyung, K.; Zhu, X.; Zhang, W.; Zheng, B.; Hu, P.; Zeng, Z.; Das, S.; Li, Y.; Chi, C.; Li, R. W.; Huang, K. W.; Ding, J.; Kim, D.; Wu, J. Dibenzoheptazethrene Isomers with Different Biradical Characters: An Exercise of Clar's Sextets Rule in Singlet Biradicaloids. *J. Am. Chem. Soc.* **2013**, *135*, 18229−18236. (e) Hu, P.; Lee, S.; Park, K. H.; Das, S.; Herng, T. S.; Gonçalves, T. P.; Huang, K.-W.; Ding, J.; Kim, D.; Wu, J. Octazethrene and Its Isomer with Different Diradical Characters and Chemical Reactivity: The Role of the Bridge Structure. *J. Org. Chem.* **2016**, *81*, 2911−2919. (f) Sun, Z.; Zheng, B.; Hu, P.; Huang, K.-W.; Wu, J. Highly Twisted 1,2:8,9-Dibenzozethrenes: Synthesis, Ground State, and Physical Properties. *ChemPlusChem* **2014**, *79*, 1549−1553. (g) Yadav, P.; Das, S.; Phan, H.; Herng, T. S.; Ding, J.; Wu, J. Kinetically Blocked Stable 5,6:12,13-Dibenzozethrene: A Laterally π-Extended Zethrene with Enhanced Diradical Character. *Org. Lett.* **2016**, *18*, 2886−2889. (h) Rudebusch, G. E.; Zafra, J. L.; Jorner, K.; Fukuda, K.; Marshall, J. L.; Arrechea-Marcos, I.; Espejo, G. L.; Ponce-Ortiz, C. J.; Gomez-Garcia, C. J.; Zakharov, L. N.; Nakano, M.; Ottosson, H.; Casado, J.; Haley, M. M. Diindeno-Fusion of an Anthracene as a Design Strategy for Stable Organic Biradicals. *Nat. Chem.* **2016**, *8*, 753−759. (i) Majewski, M. A.; Chmielewski, P. J.; Chien, A.; Hong, Y.; Lis, T.; Witwicki, M.; Kim, D.; Zimmerman, P. M.; Stępień, M. 5,10-Dimesityldiindeno[1,2-a:2′,1′-i]phenanthrene: A Stable Biradicaloid Derived from Chichibabin's Hydrocarbon. *Chem. Sci.* **2019**, *10*, 3413−3420. (j) Lu, R.-Q.; Wu, S.; Yang, L.-L.; Gao, W.-B.; Qu, H.; Wang, X.-Y.; Chen, J.-B.; Tang, C.; Shi, H.-Y.; Cao, X.-Y. Stable Diindeno-Fused Corannulene Regioisomers with Open-Shell Singlet Ground States and Large Diradical Characters. *Angew. Chem., Int. Ed.* **2019**, *58*, 7600−7605. (k) Miyoshi, H.; Miki, M.; Hirano, S.; Shimizu, A.; Kishi, R.; Fukuda, K.; Shiomi, D.; Sato, K.; Takui, T.; Hisaki, I.; Nakano, M.; Tobe, Y. Fluoreno[2,3-b]fluorene vs Indeno[2,1-*b*]fluorene: Unusual Relationship between the Number of π Electrons and Excitation Energy in m-Quinodimethane-Type Singlet Diradicaloids. *J. Org. Chem.* **2017**, *82*, 1380−1387. (l) Barker, J. E.; Frederickson, C. K.; Jones, M. H.; Zakharov, L. N.; Haley, M. M. Synthesis and Properties of Quinoidal Fluorenofluorenes. *Org. Lett.* **2017**, *19*, 5312−5315. (m) Hacker, A. S.; Pavano, M.; Wood, J. E., II; Hashimoto, H.; D'Ambrosio, K. M.; Frederickson, C. K.; Zafra, J. L.; Gómez-García, C. J.; Postils, V.; McDonald, A. R.; Casanova, D.; Frantz, D. K.; Casado, J. Fluoreno[2,1-*a*]fluorene: an *ortho*-Naphthoquinodimethane-Based System with Partial Diradical Character. *Chem. Commun.* **2019**, *55*, 14186−14189. (n) Melidonie, J.; Dmitrieva, E.; Zhang, K.; Fu, Y.; Popov, A. A.; Pisula, W.; Berger, R.; Liu, J.; Feng, X. Dipyrene-Fused Dicyclopenta[*a*,*f*]naphthalenes. *J. Org. Chem.* **2020**, *85*, 215−223.

(11) (a) Chase, D. T.; Rose, B. D.; McClintock, S. P.; Zakharov, L. N.; Haley, M. M. Indeno[1,2-*b*]fluorenes: Fully conjugated Antiaromatic Analogues of Acenes. *Angew. Chem., Int. Ed.* **2011**, *50*, 1127−1130. (b) Shimizu, A.; Tobe, Y. Indeno[2,1-*a*]fluorene: An Air-stable Orthoquinodimethane Derivative. *Angew. Chem., Int. Ed.* **2011**, *50*, 6906−6910. (c) Fix, A. G.; Deal, P. E.; Vonnegut, C. L.; Rose, B. D.; Zakharov, L. N.; Haley, M. M. Indeno[2,1-*c*]fluorene: A New Electron-Accepting Scaffold for Organic Electronics. *Org. Lett.* **2013**, *15*, 1362−1365. (d) Shimizu, A.; Kishi, R.; Nakano, M.; Shiomi, D.; Sato, K.; Takui, T.; Hisaki, I.; Miyata, M.; Tobe, Y. Indeno[2,1-*b*]fluorene: A 20-π-Electron Hydrocarbon with Very Low-Energy Light Absorption. *Angew. Chem., Int. Ed.* **2013**, *52*, 6076−6079. (e) Dressler, J. J.; Zhou, Z.; Marshall, J. L.; Kishi, R.; Takamuku, S.; Wei, Z.; Spisak, S. N.; Nakano, M.; Petrukhina, M. A.; Haley, M. M. Synthesis of the Unknown Indeno[1,2-*a*]fluorene Regioisomer: Crystallographic Characterization of Its Dianion. *Angew. Chem., Int. Ed.* **2017**, *56*, 15363−15367.

(12) (a) Tobe, Y. Non-Alternant Non-Benzenoid Aromatic Compounds: Past, Present, and Future. *Chem. Rec.* **2015**, *15*, 86−96. (b) Frederickson, C. K.; Rose, B. D.; Haley, M. M. Explorations of the Indenofluorenes and Expanded Quinoidal Analogues. *Acc. Chem. Res.* **2017**, *50*, 977−987.

(13) Nakano, M. Electronic Structure of Open-Shell Singlet Molecules: Diradical Character Viewpoint. *Top. Curr. Chem.* **2017**, *375*, 1−67.

(14) *Inter alia*: (a) Gilroy, J. B.; McKinnon, S. D. J.; Kennepohl, P.; Zsombor, M. S.; Ferguson, M. J.; Thompson, L. K.; Hicks, R. G. Probing Electronic Communication in Stable Benzene-Bridged Verdazyl Diradicals. *J. Org. Chem.* **2007**, *72*, 8062−8069. (b) Caneschi, A.; Chiesi, P.; David, L.; Ferraro, F.; Gatteschi, D.; Sessoli, R. Crystal Structure and Magnetic Properties of Two Nitronyl Nitroxide Biradicals and of Their Copper(II) Complexes. *Inorg. Chem.* **1993**, *32*, 1445−1453.

(15) (a) Hubbard, J. Electron correlations in narrow energy bands. *Proc. R. Soc. A* **1963**, *276*, 238−257. (b) Fazekas, P. *Lecture Notes on Electron Correlation and Magnetism*; World Scientific: Singapore, 1999.

(16) Gebhard, F. *The Mott Metal-Insulator Transition, Models and Methods*; Springer: Heidelberg, Germany, 1997.

(17) Knall, A.-C.; Ashraf, R. S.; Nikolka, M.; Nielsen, C. B.; Purushothaman, B.; Sadhanala, A.; Hurhangee, M.; Broch, K.; Harkin, D. J.; Novák, J.; Neophytou, M.; Hayoz, P.; Sirringhaus, H.; McCulloch, I. Naphthacenodithiophene Based Polymers—New Members of the Acenodithiophene Family Exhibiting High Mobility and Power Conversion Efficiency. *Adv. Funct. Mater.* **2016**, *26*, 6961−6969.

(18) Nakagawa, H.; Kawai, S.; Nakashima, T.; Kawai, T. Synthesis and Photochemical Reactions of Photochromic Terarylene Having a Leaving Methoxy Group. *Org. Lett.* **2009**, *11*, 1475−1478.

(19) Kubo, T.; Shimizu, A.; Sakamoto, M.; Uruichi, M.; Yakushi, K.; Nakano, M.; Shiomi, D.; Sato, K.; Takui, T.; Morita, Y.; Nakasuji, K. Synthesis, Intermolecular Interaction, and Semiconductive Behavior of a Delocalized Singlet Biradical Hydrocarbon. *Angew. Chem., Int. Ed.* **2005**, *44*, 6564−6568.

(20) Shimizu, A.; Kubo, T.; Uruichi, M.; Yakushi, K.; Nakano, M.; Shiomi, D.; Sato, K.; Takui, T.; Hirao, Y.; Matsumoto, K.; Kurata, H.; Morita, Y.; Nakasuji, K. Alternating Covalent Bonding Interactions in a One-Dimensional Chain of a Phenalenyl-Based Singlet Biradical Molecule Having Kekulé Structures. *J. Am. Chem. Soc.* **2010**, *132*, 14421−14428.

(21) Bleaney, B.; Bowers, K. D. Anomalous Paramagnetism of Copper Acetate. *Proc. R. Soc. London A* **1952**, *214*, 451−465.

(22) Shimizu, A.; Hirao, Y.; Matsumoto, K.; Kurata, H.; Kubo, T.; Uruichi, M.; Yakushi, K. Aromaticity and π-bond covalency: prominent intermolecular covalent bonding interaction of a Kekulé

DOI: 10.1021/jacs.9b11898
J. Am. Chem. Soc. 2020, 142, 1548−1555

hydrocarbon with very significant singlet biradical character. *Chem. Commun.* **2012**, *48*, 5629−5631.

DOI: 10.1021/jacs.9b11898
J. Am. Chem. Soc. 2020, 142, 1548−1555